

Research Article

Screening Antimicrobial Activity of Nickel Nanoparticles Synthesized Using *Ocimum sanctum* Leaf Extract

Chitra Jeyaraj Pandian,¹ Rameshthangam Palanivel,² and Solairaj Dhanasekaran²

¹Department of Biochemistry, Manonmaniam Sundaranar University, Tirunelveli, Tamil Nadu 627012, India

²Department of Biotechnology, Science Campus, Alagappa University, Karaikudi, Tamil Nadu 630 004, India

Correspondence should be addressed to Rameshthangam Palanivel; rameshthangam@alagappauniversity.ac.in

Received 19 October 2015; Accepted 15 February 2016

Academic Editor: Tapas Sen

Copyright © 2016 Chitra Jeyaraj Pandian et al. This is an open access article distributed under the Creative Commons Attribution License, which permits unrestricted use, distribution, and reproduction in any medium, provided the original work is properly cited.

Antimicrobial efficacy of nickel nanoparticles synthesized using leaf extract of *Ocimum sanctum* (NiGs) was investigated against pathogenic Gram-negative (*E. coli*, *K. pneumoniae*, and *S. typhi*), Gram-positive (*B. subtilis*, *S. epidermidis*) bacteria and fungi (*C. albicans*, *C. tropicalis*, *A. fumigatus*, *A. clavatus*, and *A. niger*). 100 µg/mL NiGs showed maximum antimicrobial activity against tested pathogens compared to leaf extract and antibiotics. *E. coli* (25 mm) and *C. albicans* (23 mm) exhibited higher zone of inhibition at 100 µg/mL NiGs. MIC, MBC, and MFC values of NiGs against all tested pathogens ranged between 25 and 50 µg/mL. Growth of bacterial and fungal cells (10⁵ cfu/mL) was completely inhibited at 50 µg/mL NiGs. *E. coli* and *C. albicans* have showed strong antimicrobial activity with 81% and 50% reactive oxygen species (ROS) production, 30 and 16 µg/mL protein leakage, and 95 and 82 U/L LDH leakages, respectively. Gram-negative bacteria and *Candida* species showed more sensitivity to NiGs at all concentrations tested (25–100 µg/mL) than Gram-positive bacteria and *Aspergillus* species, respectively. Microbial growth in the presence of NiGs and ascorbic acid confirmed the involvement of ROS in antimicrobial activity. Hence, NiGs induced ROS generation was attributed to the protein and LDH leakage from microbial membranes.

1. Introduction

Recent increase in microbial resistance to diverse antibiotics and uncertainties in health care cost lead to the emergence of more economical new methods to produce nanoparticles with specific physical, chemical properties and limited resistance [1]. The antimicrobial activities of nanoparticles have been attributed to their relatively smaller sizes and high amount of surface-area-to-volume ratio that facilitate interacting closely with membranes of viruses, fungi, and bacteria [2]. Antimicrobial activities of metal nanoparticles like Ag, Cu, Ni, and Co (and their oxides) have been previously reported [3]. Stabilizing and protective agents in chemical synthesis of nanoparticles interact chemically with the surface of nickel nanoparticles and modify their morphology, electronic and magnetic properties [4]. In recent years, there is an increasing emphasis on green synthesis of metal nanoparticles because of their application in utilization of nontoxic renewable chemicals and

elimination of generated waste [5]. Polymeric nanoparticles like chitin nanoparticles were also found to be low cost biodegradable material for environmental protection [6]. But the plant-mediated nanoparticles synthesis is rapid, cost-effective, ecofriendly, and safe single step method for human therapeutic use [7]. Medicinal plant *Ocimum sanctum* has been found to be highly effective in different types of animal models for antimicrobial, immunomodulatory, antistress, anti-inflammatory, antipyretic, antiasthmatic, hypoglycemic, hypotensive, and analgesic activities [8]. *O. sanctum* leaves have been reported to show strong antifungal activities and antibacterial activity [9]. Earlier studies provide substantial evidence that nanoparticles produce reactive oxygen species (ROS) in bacterial cells and ROS accumulation intracellularly regulates apoptosis [10]. Oxidative stress-induced respiratory cells damage can be determined by measuring respiratory chain lactate dehydrogenase activity in microbial cells and nanoparticles enhance protein leakage by increasing membrane permeability [11]. In our previous work [12], we have

synthesized and characterized nickel nanoparticles using leaf extracts of *Ocimum sanctum* with 1 mM of aqueous nickel nitrate. Antimicrobial activity of synthesized nickel nanoparticles was evaluated by various susceptibility assays on bacterial and fungal pathogens. The toxicity of NiGs was studied against Gram-negative (*Escherichia coli*, *Klebsiella pneumoniae*, and *Salmonella typhi*) and Gram-positive (*Bacillus subtilis*, *Staphylococcus epidermidis*) bacterial and fungal pathogens (*Candida albicans*, *Candida tropicalis*, *Aspergillus fumigatus*, *Aspergillus clavatus*, and *Aspergillus niger*). We also substantiate that NiGs induced reactive oxygen species formation destroys microbial cell membrane and its permeability leading to growth suppression and cell death.

2. Materials and Methods

2.1. Materials and Strains. *O. sanctum* leaves were collected from Karaikudi town, Tamil Nadu, India. Taxonomic identification was done by Department of Botany, Alagappa University, Karaikudi, Tamil Nadu, India.

Lyophilized cultures of *Escherichia coli* (MTCC 1682), *Klebsiella pneumoniae* (MTCC 8911), *Salmonella typhi* (MTCC 3224), *Bacillus subtilis* (MTCC 6133), *Staphylococcus epidermidis* (MTCC 7919), *Candida albicans* (MTCC 3018), *Candida tropicalis* (MTCC 6222), *Aspergillus fumigatus* (MTCC 2508), *Aspergillus clavatus* (MTCC 1323), and *Aspergillus niger* (MTCC 281) were procured from Microbial Type Culture Collection (MTCC) located in Indian Institute of Microbial Technology, Chandigarh, India. Mueller-Hinton agar media for bacteria and potato dextrose agar media for fungi were purchased from Hi-Media Laboratories, Mumbai, India. Nickel nitrate was purchased from SD Fine Chemicals Ltd., Mumbai, India. All other chemicals were purchased from Sigma-Aldrich, Mumbai, India.

2.2. Synthesis and Characterization of Nanoparticles. Nickel nanoparticles were synthesized using the leaf extract of *O. sanctum* and characterized according to our previous study [12]. Chemical interaction of compounds present in *Ocimum sanctum* leaf extract with nanoparticles and morphology of NiGs were characterized by Fourier transform infrared (FTIR) spectroscopy and transmission electron microscope (TEM), respectively.

2.3. Dose-Dependent Antimicrobial Assay. Antibacterial and antifungal assays were performed with Mueller-Hinton (MH) agar and Sabouraud dextrose (SD) agar medium, respectively. Bacterial and fungal cultures were prepared to 0.5 McFarland standards prior to the assay. Antimicrobial activity of NiGs was evaluated by disc diffusion assay against the Gram-negative bacteria (*E. coli*, *K. pneumoniae*, and *S. typhi*), Gram-positive bacteria (*B. subtilis*, *S. epidermidis*), and fungi (*C. albicans*, *C. tropicalis*, *A. clavatus*, *A. fumigatus*, and *A. niger*). Pure microbial cultures were subcultured on nutrient agar and uniformly swabbed on individual plates. 20 μ L of NiGs at different concentrations (25, 50, and 100 μ g/mL) was impregnated to 6 mm filter paper discs, dried, and placed on the culture plate. Bacterial and fungal cultures were incubated

at 37°C for 24 h and 48 h, respectively [13]. Antimicrobial activities were studied by the diameter of zone of inhibition. Deionized water (as control) and leaf extract were used to compare the antimicrobial activity of NiGs.

2.4. Minimum Inhibitory Concentration (MIC), Minimum Bactericidal Concentration (MBC), and Minimum Fungicidal Concentration (MFC) Assay. 100 μ L of NiGs in serially descending concentrations 200 to 1 μ g/mL was added to microtitre plates with 100 μ L MH broth for bacterial or 100 μ L SD broth for fungal assays. Dilutions were done by twofold serial dilution and 100 μ L of bacterial and fungal samples was inoculated to respective wells. Bacterial and fungal plates were incubated for 24 h and 48 h, respectively, at 37°C [13] and optical densities were determined at 600 nm using microplate reader. Antibiotics (amoxicillin (Amx) and nystatin (Nys)) were used to compare the bactericidal and fungicidal activity of NiGs.

MBC and MFC were determined by subculturing 2 μ L of above MIC serial dilution after 24 h of incubation in respective wells containing 100 μ L of broth per well. Bacterial and fungal colonies were quantified by further incubation for 24 h and 48 h, respectively, at 37°C. MBC and MFC were the lowest concentration of nanoparticles or antibiotics that prevented the growth of bacterial and fungal colonies on solid media, respectively [14].

2.5. Determination of Microbial Growth Kinetics in the Presence of NiGs. Microbial growth rate was observed by inoculating the microtitre plates with MH and SD broth containing 10⁵ colony forming units (cfu) per mL of bacterial or fungal pathogens, respectively, and loaded with varying concentrations of nanoparticles (0, 25, 50, and 100 μ g/mL). The plates were incubated at 37°C and shaken at 180 rpm. After inoculation, the optical density (OD) at 600 nm [15] was serially monitored at every 3 h interval till 24 h and every 6 h interval till 48 h for bacterial and fungal pathogens, respectively.

2.6. Detection of Reactive Oxygen Species (ROS). Reactive oxygen species produced in microbial cells were determined by 2',7' dichlorofluorescein diacetate (DCFDA). Intracellular esterase cleaves fluorescence based probe dichloro-dihydro-fluorescein diacetate (DCFH-DA) to polar impermeable non-fluorescent molecule that accumulates intracellularly and its subsequent oxidation yields highly fluorescent product 2',7' dichlorofluorescein (DCF) which was monitored by increase in fluorescence. 10⁵ cfu/mL bacterial and fungal pathogens were treated with 0, 25, 50, and 100 μ g/mL NiGs and incubated at 37°C for 6 h and 24 h, respectively. After incubation, the cultures were centrifuged at 5000 rpm for 10 min at 4°C. The supernatant was treated with 100 μ M DCFDA for 1 h and the ROS formed (fluorescence intensity of DCF) was determined at 488 nm excitation wavelength and 535 nm emission wavelength using fluorescence spectrophotometer [11].

2.7. Assaying the Effect of NiGs on Protein Leakage. Bradford method was performed to analyze the protein leakage in the microbial cells. The bacterial and fungal pathogens (10^5 cfu/mL) were treated with 0, 25, 50, and 100 $\mu\text{g/mL}$ NiGs for 6 h and 24 h, respectively. After incubation, the contents were centrifuged at 5000 rpm for 5 min and supernatant was collected. 200 μL of supernatant from each sample was mixed with 800 μL of Bradford reagent and incubated for 10 min in dark at 37°C . The optical density was determined at 595 nm with bovine serum albumin as standard [16].

2.8. Assaying the Effect of NiGs on Lactate Dehydrogenase (LDH) Activity. The cytoplasmic enzyme LDH release and cell membrane instability were studied as per the procedure reported by Arokiyaraj et al. (2014) [17]. 100 μL of supernatant from each microbial culture treated with different concentrations of NiGs (0, 25, 50, and 100 $\mu\text{g/mL}$) was added to the reaction mixture containing 0.5 mL of 100 mM pyruvate, 5 mg NADH in 20 mL of 500 mM potassium phosphate buffer, and pH 7.5 at 30°C . Absorbance (A) was recorded for 0.5 to 5 min and relative change in the absorbance per minute ($\Delta A/\text{min}$) was calculated at 340 nm using UV-visible spectrophotometer. LDH activity was expressed in international unit (U/L) which is the amount of enzyme that reduces 1 μM of NAD per min at specific temperature:

$$U/L = \frac{\Delta A/\text{min} \times TV \times 1000}{d} \times \epsilon \times SV, \quad (1)$$

where TV is the total reaction volume, 1000 is the conversion of U/mL into U/L, d is the light path in cm, ϵ is the absorptivity of NADH in mM, and SV is the sample volume in mL.

2.9. Determining the Effect of Antioxidant on Microbicidal Activity of NiGs. The involvement of free radicals formation by NiGs was confirmed using antioxidant ascorbic acid that acts as scavenger of free radicals [18]. MH and SD broth with 10^5 cfu/mL bacterial and fungal samples were supplemented with 100 $\mu\text{g/mL}$ NiGs and 10 mM ascorbic acid and were shaken at 180 rpm at 37°C . The growth rate at OD 600 nm was determined at regular intervals till 24 h and 72 h of incubation for bacterial and fungal pathogens, respectively.

2.10. Statistical Analysis. All the experiments were performed in triplicate and the data were expressed as the mean \pm standard deviation (SD). Error bars represent standard deviations of duplicate experiments.

3. Results and Discussion

3.1. Synthesis and Characterization of NiGs. NiGs were synthesized using *O. sanctum* leaf extract and the physicochemical properties were characterized (FTIR and TEM) and reported in our previous work [12].

The FTIR spectrum of NiGs in our previous study [12] evidenced the presence of functional groups such as O–H stretching carboxylic acid, C–N or C–C triple bond, N–H bend primary amines, C–C stretch aliphatic amines, and C–N

TABLE 1: Zone of inhibition (mean \pm SD) of NiGs against bacterial and fungal pathogens.

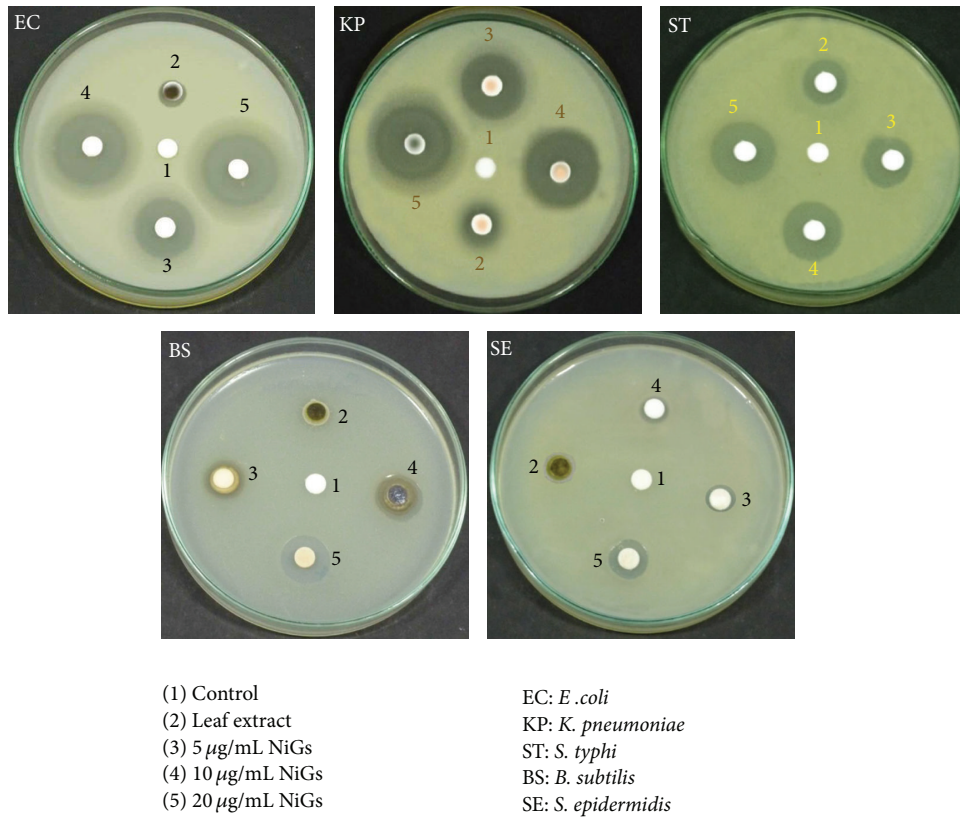
Bacteria	Zone of inhibition (mm)			
	Leaf extract	NiGs ($\mu\text{g/mL}$)		
		25	50	100
<i>E. coli</i>	9.0 \pm 0.2	15.3 \pm 0.3	19.2 \pm 0.5	25.1 \pm 0.1
<i>K. pneumoniae</i>	7.8 \pm 0.9	9.5 \pm 0.5	18.1 \pm 0.7	23.3 \pm 0.7
<i>S. typhi</i>	5.8 \pm 0.3	8.0 \pm 1.4	18.3 \pm 0.3	20.2 \pm 0.3
<i>B. subtilis</i>	5.2 \pm 0.5	7.1 \pm 0.8	16.5 \pm 0.2	19.5 \pm 0.5
<i>S. epidermidis</i>	3.9 \pm 0.6	5.2 \pm 0.3	16.0 \pm 0.8	18.6 \pm 0.9
Fungi	Leaf extract	NiGs ($\mu\text{g/mL}$)		
		25	50	100
	<i>C. albicans</i>	7.8 \pm 0.1	14.5 \pm 0.4	18.2 \pm 0.7
<i>C. tropicalis</i>	5.2 \pm 0.6	12.4 \pm 0.8	14.4 \pm 0.2	21.6 \pm 0.9
<i>A. clavatus</i>	4.5 \pm 0.3	10.4 \pm 0.1	14.3 \pm 0.1	18.7 \pm 0.5
<i>A. fumigatus</i>	3.7 \pm 0.4	8.5 \pm 0.3	10.7 \pm 0.9	15.5 \pm 0.6
<i>A. niger</i>	2.5 \pm 0.1	6.2 \pm 0.5	7.5 \pm 0.5	12.4 \pm 0.1

rock in alkanes indicating the interaction of metabolites and proteins in the *O. sanctum* leaf extract with the NiGs. These interacting biological molecules could have been involved in the formation and stabilization of NiGs in aqueous medium. This is in concurrence with the findings by Mallikarjuna et al. [19] who have reported that the amino acid residues or proteins in *O. sanctum* leaf extract can strongly bind to silver nanoparticles, preventing its agglomeration and hence stabilizing the nanoparticles.

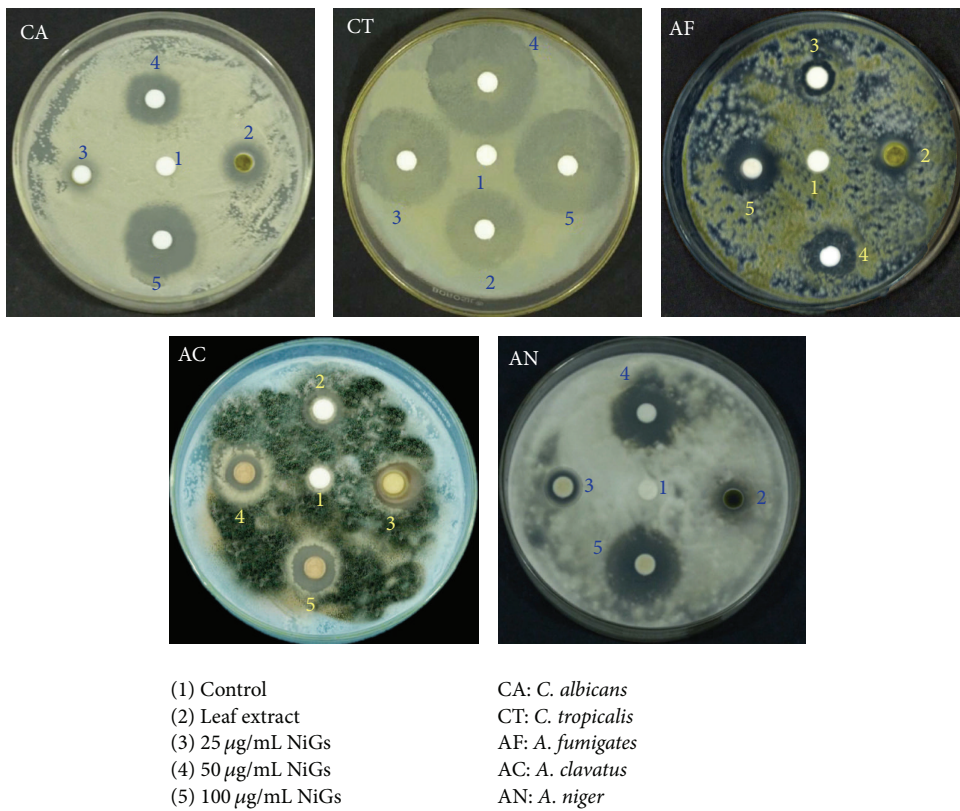
TEM micrograph of the NiGs in our previous study [12] showed that the shape of the NiGs was almost spherical and the distribution of the particles was narrow. The diameter of the sample ranged between 12 and 36 nm and shows a certain extent of particles agglomeration [12]. Our study is in good agreement with previous study by Govindasamy et al. [20] and Wang et al. [21] who have reported that the varied shape (irregular polygonal, cylindrical, and spherical) of nickel nanoparticles with particle agglomeration is due to magnetic interaction and polymer adherence between the particles, respectively.

3.2. Antibacterial and Antifungal Activity of NiGs. In disc diffusion assay, the suppression of bacterial growth was determined in Petri plates loaded with 25–100 $\mu\text{g/mL}$ NiGs after 24 h at 37°C (Figure 1(a) and Table 1). Zone of inhibition was not observed in control plates loaded with deionized water while leaf extract has showed higher growth inhibition. Diameter of inhibition zone ranged from 15.3 to 25.1 mm, 9.5 to 23.3 mm, 8 to 20.2 mm, 7.1 to 19.5 mm, and 5.2 to 18.6 mm in *E. coli*, *K. pneumoniae*, *S. typhi*, *B. subtilis*, and *S. epidermidis*, respectively, with increase in NiGs concentration from 25 to 100 $\mu\text{g/mL}$. It is evident from Figure 1(a) that size of inhibition zone increases linearly with increase in NiGs concentration (25–100 $\mu\text{g/mL}$).

The presence of inhibition zone in Figure 1(b) confirmed the antifungal activity of NiGs. The size of inhibition zone differed with the type of fungal pathogen and concentration of NiGs. Maximum antifungal activity was observed



(a)



(b)

FIGURE 1: Zone of inhibition of (a) bacterial and (b) fungal pathogens treated with NiGs.

TABLE 2: MIC, MBC, and MFC (mean \pm SD) of NiGs against bacterial and fungal pathogens.

Bacteria	Leaf extract ($\mu\text{g/mL}$)		Amoxicillin ($\mu\text{g/mL}$)		NiGs ($\mu\text{g/mL}$)	
	MIC	MBC	MIC	MBC	MIC	MBC
<i>E. coli</i>	50 \pm 0.3	50 \pm 0.1	25 \pm 0.3	50 \pm 1.3	25 \pm 0.3	25 \pm 2.4
<i>K. pneumoniae</i>	50 \pm 0.1	50 \pm 0.0	50 \pm 2.0	50 \pm 0.1	25 \pm 2.8	25 \pm 0.7
<i>S. typhi</i>	50 \pm 1.0	100 \pm 0.8	50 \pm 0.4	100 \pm 0.0	25 \pm 0.2	25 \pm 1.6
<i>B. subtilis</i>	100 \pm 0.5	100 \pm 1.3	50 \pm 1.7	100 \pm 0.2	50 \pm 0.2	50 \pm 0.2
<i>S. epidermidis</i>	100 \pm 0.2	100 \pm 0.6	50 \pm 0.2	100 \pm 0.1	50 \pm 0.5	50 \pm 0.1
Fungi	Leaf extract ($\mu\text{g/mL}$)		Nystatin ($\mu\text{g/mL}$)		NiGs ($\mu\text{g/mL}$)	
	MIC	MFC	MIC	MFC	MIC	MFC
<i>C. albicans</i>	50 \pm 0.2	50 \pm 0.4	50 \pm 0.1	50 \pm 2.1	25 \pm 1.4	50 \pm 0.0
<i>C. tropicalis</i>	50 \pm 0.1	100 \pm 0.1	50 \pm 0.7	100 \pm 0.8	25 \pm 0.7	50 \pm 0.1
<i>A. clavatus</i>	100 \pm 2.5	100 \pm 0.9	50 \pm 0.0	100 \pm 1.2	50 \pm 2.5	50 \pm 0.5
<i>A. fumigatus</i>	100 \pm 0.0	100 \pm 1.3	100 \pm 0.3	100 \pm 0.0	50 \pm 1.0	50 \pm 1.2
<i>A. niger</i>	100 \pm 0.9	100 \pm 0.2	100 \pm 1.0	100 \pm 0.3	50 \pm 0.8	50 \pm 0.6

at 100 $\mu\text{g/mL}$ NiGs for *C. albicans* (23.1 mm), *C. tropicalis* (21.6 mm), *A. clavatus* (18.7 mm), *A. fumigatus* (15.5 mm), and *A. niger* (12.4 mm). Zone of inhibition was not observed in plates loaded with deionized water for tested fungal pathogens. Leaf extract showed minimal antifungal activity with inhibition zone diameter of 7.8, 5.2, 4.5, 3.7, and 2.5 mm for *C. albicans*, *C. tropicalis*, *A. clavatus*, *A. fumigatus*, and *A. niger*, respectively. Maximum antimicrobial activity was observed at 100 $\mu\text{g/mL}$ NiGs for all tested pathogens at lower concentrations (25, 50 $\mu\text{g/mL}$). Therefore it is clear from the data that the antibacterial and antifungal activities are dose-dependent.

Disc diffusion study of NiGs confirmed that bacterial and fungal growth inhibition was dose-dependent with maximum activity at 100 $\mu\text{g/mL}$ and it could be due to the release of nickel ions from NiGs that increased membrane permeability and ROS generation leading to cell death. This observation is in good agreement with the earlier antibacterial reports for zinc oxide nanoparticles at 2 to 12 mM concentration [22] and for silver nanoparticles at concentration 10 to 150 μM [14, 23].

3.3. Minimum Inhibitory Concentration (MIC) and Minimum Microbicidal Concentration (MBC/MFC). MIC of NiGs was studied to determine the lowest concentration that could completely inhibit visible growth of bacterial and fungal pathogens. Antimicrobial activity of NiGs in terms of MIC, MBC, and MFC is shown in Table 2. Both inhibitory and bactericidal concentrations of leaf extract were found to be 100 $\mu\text{g/mL}$ for Gram-positive bacteria (*B. subtilis* and *S. epidermidis*) and *Aspergillus* species (*A. clavatus*, *A. fumigatus*, and *A. niger*) while 50 $\mu\text{g/mL}$ was observed for Gram-negative bacteria (*E. coli*, *K. pneumoniae*, and *S. typhi*) and *Candida* species (*C. albicans* and *C. tropicalis*).

25 $\mu\text{g/mL}$ NiGs were the minimum inhibitory concentration against all bacterial pathogens. 25 $\mu\text{g/mL}$ NiGs showed

bactericidal activity against *E. coli*, *K. pneumoniae*, and *S. typhi* while 50 $\mu\text{g/mL}$ NiGs exhibited bactericidal activity against *B. subtilis* and *S. epidermidis*. This data is comparable with the antibiotic amoxicillin which showed inhibitory activity at 50 $\mu\text{g/mL}$ for all bacterial pathogens and bactericidal activity of 100 $\mu\text{g/mL}$ for *S. typhi*, *B. subtilis*, and *S. epidermidis*. 25 $\mu\text{g/mL}$ amoxicillin has showed bactericidal activity against *E. coli*, *K. pneumoniae*, *S. typhi*, *B. subtilis*, and *S. epidermidis*. Therefore the minimum inhibitory concentration (25 $\mu\text{g/mL}$) and minimum bactericidal concentration (50 $\mu\text{g/mL}$) of NiGs were much lower than the antibiotics.

Among fungal pathogens maximum sensitivity was observed in *C. albicans* and *C. tropicalis* has showed MIC and MFC of NiGs at 25 and 50 $\mu\text{g/mL}$, respectively. Minimum inhibitory and fungicidal concentration of NiGs were found to be 50 $\mu\text{g/mL}$ for *A. clavatus*, *A. fumigatus*, and *A. niger*. MIC and MFC of antibiotic nystatin were observed at 50 and 100 $\mu\text{g/mL}$ for most of the fungal pathogens tested. Gram-positive bacteria, *A. clavatus*, *A. fumigatus*, and *A. niger*, have showed MIC, MBC, and MFC of NiGs at 50 $\mu\text{g/mL}$. But Gram-negative bacteria, *C. albicans* and *C. tropicalis*, have showed higher sensitivity to NiGs at lower concentration (25 $\mu\text{g/mL}$). *S. typhi* and *C. tropicalis* recorded higher MBC and MFC (100 $\mu\text{g/mL}$), respectively, for both leaf extract and antibiotics. Higher antimicrobial activity was observed in NiGs than antibiotics and leaf extract for all the tested pathogens. No significant antibacterial and antifungal activities were observed at NiGs concentrations less than 25 $\mu\text{g/mL}$. Gram-negative bacteria and *Candida* species showed relatively higher sensitivity to all tested antimicrobial agents (NiGs, antibiotics, and leaf extract) than Gram-positive bacteria and *Aspergillus* species, respectively. It is clear from the results that NiGs have enhanced inhibitory, bactericidal, and fungicidal activities.

Higher MIC and MBC values of NiGs in Gram-positive (*B. subtilis* and *S. epidermidis*) pathogens than in Gram-negative bacteria (*E. coli*, *K. pneumoniae* and *S. typhi*) are

TABLE 3: Comparison of the antimicrobial activity of NiGs with silver nanoparticles.

Organism	Antimicrobial effect (MIC)		Size (silver nanoparticles)	Ref. (silver nanoparticles)
	NiGs (size: 12–36 nm) (present study)	Silver nanoparticles		
<i>E. coli</i>	25 $\mu\text{g}/\text{mL}$	75 $\mu\text{g}/\text{mL}$	21 nm	[2]
<i>K. pneumoniae</i>	25 $\mu\text{g}/\text{mL}$	11 $\mu\text{g}/\text{mL}$	11–75 nm	[34]
<i>S. typhi</i>	25 $\mu\text{g}/\text{mL}$	75 $\mu\text{g}/\text{mL}$	21 nm	[2]
<i>B. subtilis</i>	50 $\mu\text{g}/\text{mL}$	70 $\mu\text{g}/\text{mL}$	20 nm	[35]
<i>S. epidermidis</i>	50 $\mu\text{g}/\text{mL}$	31.25 $\mu\text{g}/\text{mL}$	10–50 nm	[36]
<i>C. albicans</i>	25 $\mu\text{g}/\text{mL}$	0.5 mg/mL	10–30 nm	[37]
<i>C. tropicalis</i>	25 $\mu\text{g}/\text{mL}$	0.84 mg/L	25 nm	[38]
<i>Aspergillus sp.</i>	50 $\mu\text{g}/\text{mL}$	40 $\mu\text{g}/\text{mL}$	18 nm	[39]
<i>A. fumigatus</i>	50 $\mu\text{g}/\text{mL}$	8 $\mu\text{g}/\text{mL}$	20 nm	[40]
<i>A. niger</i>	50 $\mu\text{g}/\text{mL}$	75 $\mu\text{g}/\text{mL}$	20 nm	[41]

due to thick peptidoglycan layer in Gram-positive bacteria that have defended the easy penetration of nanoparticles through the cell membrane. Similarly, Arokiyaraj et al. [17] also reported higher MIC values of green synthesized silver nanoparticles (25 $\mu\text{g}/\text{mL}$) against Gram-positive bacteria than Gram-negative bacteria (6.25 $\mu\text{g}/\text{mL}$). Higher MIC and MFC values of NiGs in *A. clavatus*, *A. fumigatus*, and *A. niger* than in *C. albicans*, *C. tropicalis* in the present study are due to spore producing and filamentous nature of *Aspergillus* species (*A. clavatus*, *A. fumigatus*, and *A. niger*) that decreased fungi's sensitivity to NiGs. This observation is in agreement with previous reports [13] on antimicrobial properties of biosynthesized silver nanoparticles against *S. aureus*, *S. epidermidis*, *E. coli*, *A. niger*, and *C. albicans*. Enhanced MIC, MBC, and MFC of NiGs compared to antibiotics and leaf extract are due to nickel nanoparticle's larger surface to volume ratio and its penetration to cell membrane. This observation confirmed the earlier findings on antifungal activity [24] and antibacterial activity [25] of silver nanoparticles against *C. albicans* and of *E. coli*, respectively.

The antimicrobial activity (MIC) of NiGs was compared with the previously reported antimicrobial studies of silver nanoparticles (Table 3). NiGs showed better antimicrobial activity when compared to silver nanoparticles of similar particle size. Antimicrobial effectiveness of green synthesized metal nanoparticles depends on particle dosage, treatment time, and synthesis methods [14]. This could be the reason for higher antimicrobial activity of NiGs than silver nanoparticles. Variation in antimicrobial activity of antimicrobial activity of NiGs compared to silver nanoparticles of similar size could be mainly attributed to the differences in experimental conditions, shape, and crystal quality of the nanoparticles as reported in earlier study by Pang et al. [26].

3.4. Growth Curves of Microbial Cells Treated with Different Concentrations of NiGs. Bacterial growth curves in Figure 2 clearly demonstrated the inhibition of bacterial growth at all tested concentrations of NiGs (25–100 $\mu\text{g}/\text{mL}$). Culture medium without NiGs has not shown any inhibition of

growth and also reached stationary phase after 24 h. However, complete inhibition was obtained at 50 and 100 $\mu\text{g}/\text{mL}$ NiGs for both Gram-positive (*B. subtilis* and *S. epidermidis*) and Gram-negative bacteria (*E. coli*, *K. pneumoniae*, and *S. typhi*). 25 $\mu\text{g}/\text{mL}$ NiGs could slightly inhibit growth of bacteria but were not sufficient to outpace the reproduction of bacterial cells. From the results, it is evidenced that the bactericidal activity of NiGs increased with increasing NiGs concentration. NiGs showed faster inhibition of growth in *E. coli*, *K. pneumoniae*, and *S. typhi* than *B. subtilis* and *S. epidermidis*. Maximum inhibition was observed in *E. coli* at 100 $\mu\text{g}/\text{mL}$ NiGs.

Inhibitory effects of NiGs on the growth and reproduction of fungal pathogens with respect to concentration are shown in Figure 3. In the absence of NiGs, growth of both tested *Candida* species (*C. albicans* and *C. tropicalis*) and *Aspergillus* species (*A. clavatus*, *A. fumigatus*, and *A. niger*) reached exponential phase rapidly. However when exposed to 25 $\mu\text{g}/\text{mL}$ NiGs, growth lagged for longer hours (9 h and 24 h for bacterial and fungal pathogens, resp.). Further increasing NiGs concentration to 50 $\mu\text{g}/\text{mL}$ suppressed the fungal growth while 100 $\mu\text{g}/\text{mL}$ NiGs completely inhibited the growth of fungal pathogens. 100 $\mu\text{g}/\text{mL}$ NiGs showed maximum inhibition in *C. albicans* while the effect was less at lower concentrations (25, 50 $\mu\text{g}/\text{mL}$). Therefore, complete growth inhibition of bacterial pathogens was at 50 $\mu\text{g}/\text{mL}$ NiGs while at 100 $\mu\text{g}/\text{mL}$ for fungal pathogens.

Faster inhibition of growth and reproduction of bacterial and fungal pathogens at 100 $\mu\text{g}/\text{mL}$ than 25 and 50 $\mu\text{g}/\text{mL}$ NiGs is due to the availability of few nanoparticles and nickel ions for inhibition. Decreased antimicrobial activity at lower NiGs concentration is due to the availability of few NiGs for growth inhibition as discussed by Sawai [27] for antibacterial activities of metallic oxide (ZnO, MgO, and CaO) powders against *S. aureus* and *E. coli*. Microbicidal activity of NiGs is also due to the electrostatic interaction between positively charged nickel ions and negatively charged microbial cell membranes. These observations are in concurrence with earlier antimicrobial study [16] of zinc oxide nanoparticles against *S. enterica* and *C. albicans*.

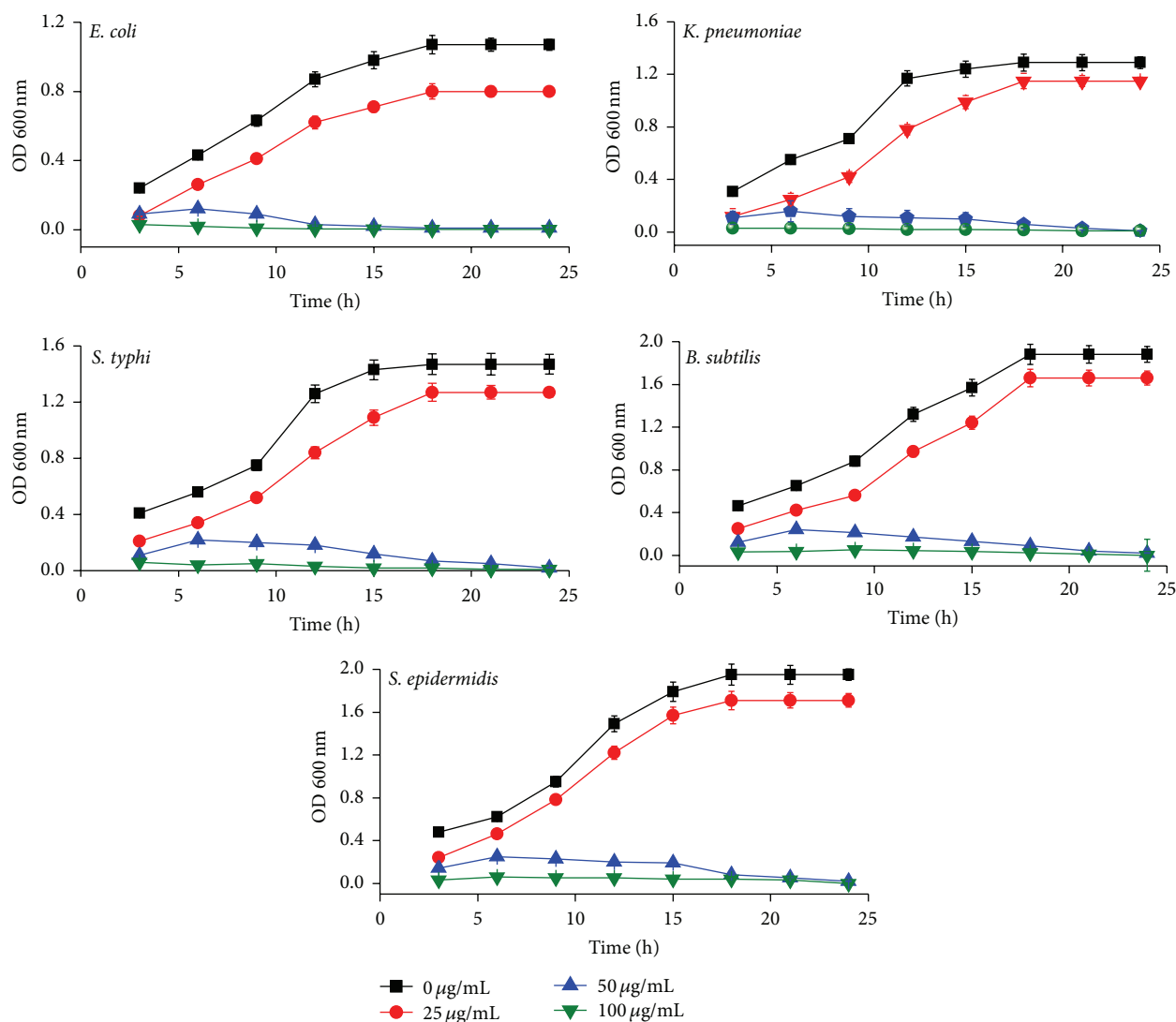


FIGURE 2: Growth curves of bacterial cells exposed to different concentrations of NiGs.

3.5. NiGs Induced Reactive Oxygen Species (ROS) Generation. Reactive oxygen species (ROS) are the natural byproducts of the metabolism [28]. Induction of ROS synthesis leads to the formation of highly reactive radicals that destroy the cells [29] by damaging cell membranes, proteins, DNA, and intracellular system [11]. Figures 4(a) and 4(b) showed continuous generation of ROS in bacterial and fungal pathogens at all tested concentrations of NiGs. ROS generated by NiGs was concentration-dependent that increased with the increasing NiGs concentration from 25 to 100 µg/mL. NiGs at 100 µg/mL generated nearly three times higher ROS in *E. coli*, *K. pneumoniae*, *S. typhi*, *B. subtilis*, and *S. epidermidis* than at lower concentration (25 µg/mL). *E. coli* and *K. pneumoniae* have showed 81 and 71% ROS generation, respectively, while *S. epidermidis* has showed minimal (50%) generation of ROS at 100 µg/mL NiGs.

Similarly ROS generation at 100 µg/mL NiGs was two times higher than in lower concentration (25 µg/mL) for all tested fungal pathogens. ROS generation was not observed

in both bacterial and fungal control plates without NiGs. Among fungal pathogens treated with NiGs, *C. albicans* and *C. tropicalis* showed maximum ROS production while *A. niger* recorded minimal (32%) production of ROS. Therefore, ROS generation was dependent on NiGs concentration and maximum ROS production was observed in Gram-negative bacteria (65% to 80%) and in *Candida* species (47 to 50%).

Increased generation of ROS from bacterial and fungal cells treated with NiGs at all varying concentrations is due to the reaction of NiGs with water forming ROS (hydrogen peroxide H_2O_2) that damages membrane proteins and permeability. Similar destruction of bacteria due to H_2O_2 generated by titanium oxide nanoparticles-biofilm interfaces was earlier discussed by Thirunavukkarasu et al. (2014) [30].

3.6. Effect of NiGs on Protein Leak from Microbial Cell Membranes. Figures 5(a) and 5(b) showed the enhanced leakage of intracellular proteins from microbial membranes into the extracellular medium at varying concentrations of

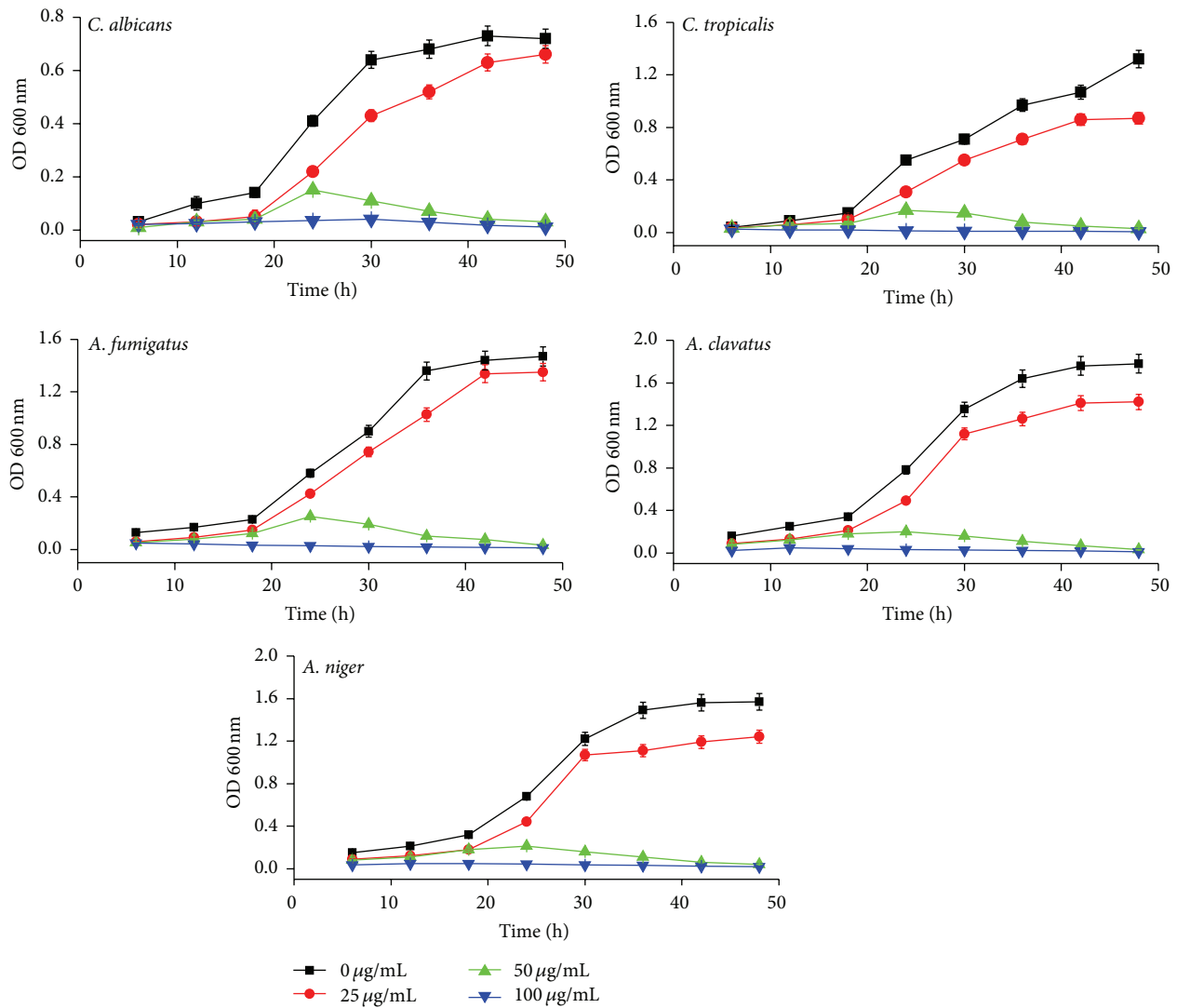


FIGURE 3: Growth curves of fungal cells exposed to different concentrations of NiGs.

NiGs (25, 50, and 100 µg/mL). No significant protein leakage from bacterial and fungal cells was detected in control. Protein leakage from NiGs treated bacterial and fungal cells increased with NiGs concentration from 25 to 100 µg/mL for a contact period of 6 h and 24 h, respectively, with maximum leak at 100 µg/mL NiGs.

At 100 µg/mL NiGs, the amount of protein leakage was up to 30, 27, 24, 19, and 14 µg/mL (Figure 5(a)) for *E. coli*, *K. pneumoniae*, *S. typhi*, *B. subtilis*, and *S. epidermidis*, respectively. Protein leakage from *E. coli*, *K. pneumoniae*, *S. typhi*, *B. subtilis*, and *S. epidermidis* membranes ranged from 19 to 26, 15 to 24, 14 to 23, 10 to 16, and 8 to 12 µg/mL, respectively, at 25–50 µg/mL NiGs. The results suggested that NiGs could accelerate leakage of protein from bacterial cytoplasm and highest leakage (30 µg/mL) was observed in *E. coli*.

Similarly, elevated protein leakage was observed in all tested fungal pathogens treated with NiGs (Figure 5(b)). Protein leakage from *C. albicans*, *C. tropicalis*, *A. clavatus*,

A. fumigatus, and *A. niger* ranged from 11 to 16, 11 to 15, 9 to 13, 8 to 13, and 5 to 11 µg/mL, respectively, at 25–100 µg/mL NiGs. *C. albicans* has showed highest protein leakage (16 µg/mL) compared to other fungal pathogens.

A similar phenomenon of ROS induced oxidative stress-induced leakage of cellular contents from microbial cell membranes treated with zinc oxide nanoparticles and silver nanoparticles was discussed elsewhere [11, 31].

3.7. Effect of NiGs on Lactate Dehydrogenase (LDH) Activity.

The effect of NiGs on lactate dehydrogenase, an important cytoplasmic enzyme, is represented in Figures 6(a) and 6(b). Significantly higher leakage of intracellular LDH into extracellular medium was observed in both bacterial (43–95 U/L) (Figure 6(a)) and fungal (48–82 U/L) (Figure 6(b)) cells treated with NiGs than control group. LDH leakage into extracellular medium increased with increase in NiGs concentration from 25 to 100 µg/mL. The LDH leakage from *E. coli*, *K. pneumoniae*, *S. typhi*, *B. subtilis*, and *S. epidermidis*

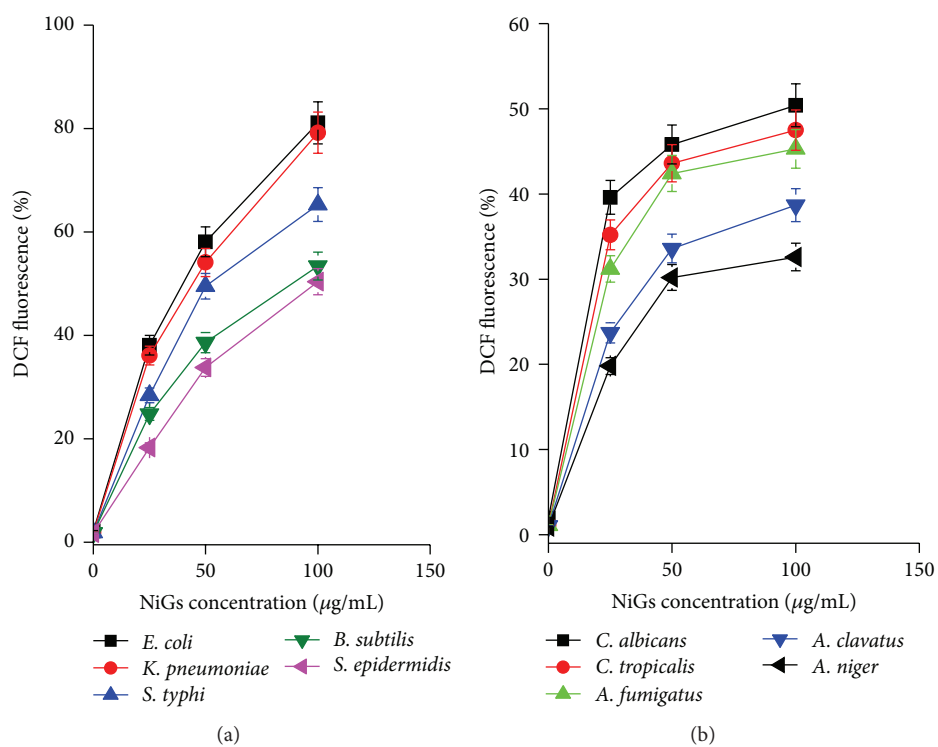


FIGURE 4: Formation of ROS in (a) bacterial and (b) fungal cells exposed to different concentrations of NiGs.

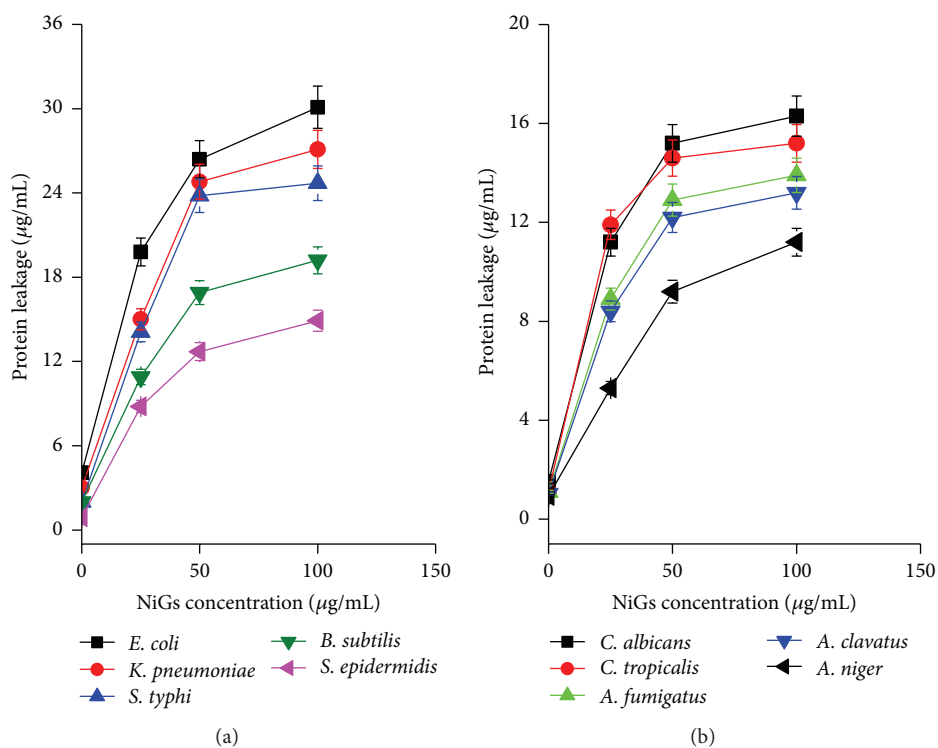


FIGURE 5: Leakage of proteins from (a) bacterial and (b) fungal cells exposed to different concentrations of NiGs.

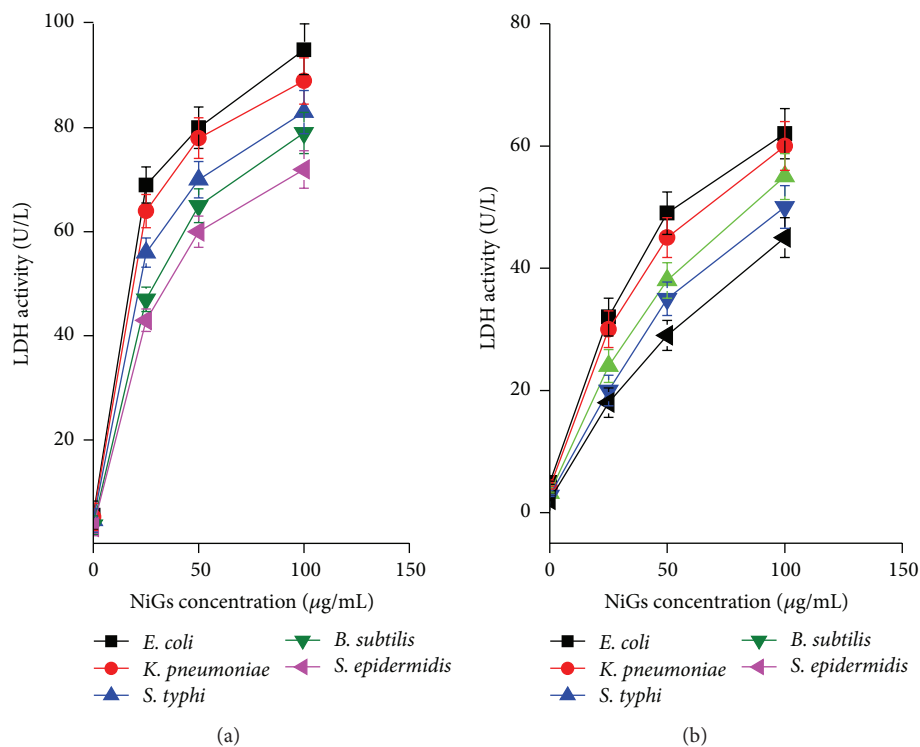


FIGURE 6: LDH leakage of (a) bacterial and (b) fungal cells exposed to different concentrations of NiGs.

in the absence of NiGs (control) was 55, 52, 45, 36, and 32 U/L, respectively. However the cells treated with 25–100 µg/mL NiGs showed higher LDH leakage ranging from 69 to 95, 64 to 89, 56 to 83, 47 to 79, and 43 to 72 U/L for *E. coli*, *K. pneumoniae*, *S. typhi*, *B. subtilis*, and *S. epidermidis*. The maximum LDH leakage (95 U/L) was observed in *E. coli* compared to other bacterial pathogens.

LDH activity of *C. albicans*, *C. tropicalis*, *A. clavatus*, *A. fumigatus*, and *A. niger* at 25–100 µg/mL NiGs was found to be 69–95, 64–89, 56–83, 47–79, and 43–72 U/L, respectively, when compared with their respective control (55, 52, 45, 36, and 32 U/L). Increase in LDH leakage with increase in NiGs concentration suggested that the NiGs enhanced the leakage of intracellular LDH.

Enhanced leakage of proteins from NiGs treated bacterial and fungal cell membranes into culture medium is due to generation of free radicals from NiGs surface that induced membrane damage and leaked membrane and cellular proteins as discussed elsewhere [32].

3.8. Effect of Antioxidant on Microbicidal Activity of NiGs. The involvement of ROS in antimicrobial activity of NiGs was confirmed by using antioxidant ascorbic acid to scavenge the ROS produced by NiGs. The protective activity of 10 mM ascorbic acid was observed (Figures 7(a) and 7(b)) against microbicidal activity of NiGs against tested pathogens. Pathogens treated with 100 µg/mL NiGs (Figures 3 and 4) have not showed any growth due to ROS formation. However, in the presence of ascorbic acid both bacterial and fungal pathogens exhibited growth similar to the control

(Figures 3 and 4). Growth curves of bacterial and fungal pathogens in Figures 7(a) and 7(b) confirmed that ascorbic acid was able to protect the cells completely from toxicity of NiGs. It is evidenced from the study that ROS was involved in the microbicidal activity of NiGs and ascorbic acid prevented this antimicrobial activity by scavenging the generated ROS. Growth curves of all tested bacterial and fungal pathogens in the presence of 100 µg/mL NiGs and 10 mM ascorbic acid were similar to the control and this is due to the free radical scavenging activity of ascorbic acid.

3.9. Mechanism of Antimicrobial Activity of NiGs. Figure 8 summarizes the interaction of NiGs with microbial cells. The antimicrobial activity of nickel nanoparticles relies on generation of ROS and release of nickel ions Ni (II). Diffusion and endocytosis of NiGs followed by nickel nanoparticle's accumulation in cell membrane alter membrane permeability and destroy membrane proteins. NiGs react with water forming ROS that penetrate the cell membrane causing protein disruption and cell membrane damage with subsequent leakage of cellular contents. Dissolution of Ni (II) ions and free radicals interrupt electron transport in the microbial cell resulting in cell death. These observations are in good agreement with earlier reports [19, 33] for antimicrobial activity of silver nanoparticles.

4. Conclusions

Green synthesis of nanoparticles provides more advancement in pharmaceutical and biomedical applications than chemical

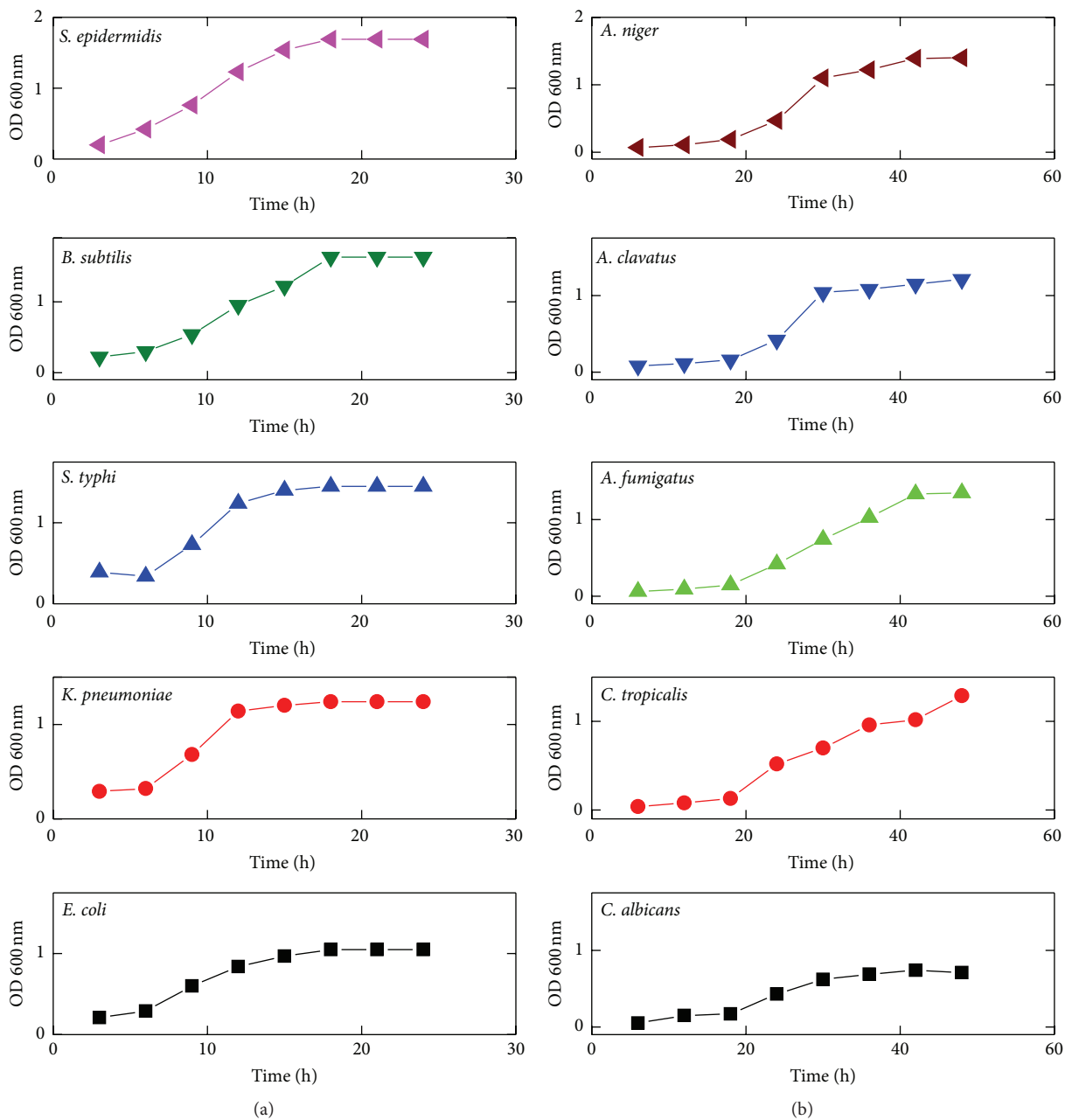


FIGURE 7: Effect of ascorbic acid on (a) bactericidal and (b) fungicidal activity of NiGs.

and physical methods due to their cost-effectiveness and ecofriendliness. To overcome the increasing drug resistance, public health problems, and adverse reactions, there is an utmost need to develop novel antimicrobial agents. Nickel nanoparticles were synthesized from leaf extract of *O. sanctum* and characterized as described in our previous study [12]. Among tested pathogens Gram-negative bacteria (*E. coli*, *K. pneumoniae*, and *S. typhi*) and *Candida* species (*C. albicans*, *C. tropicalis*) showed higher growth inhibition and microbicidal activity when treated with NiGs than Gram-positive bacteria (*B. subtilis* and *S. epidermidis*) and *Aspergillus* species

(*A. clavatus*, *A. fumigatus*, and *A. niger*), respectively. Enhanced antimicrobial activity of NiGs was attributed to the active formation of ROS that led to the loss of cellular proteins and LDH through damaged cell membrane resulting in cell death. In conclusion, the present study suggested that ROS generated from the surface of NiGs interacted and damaged the cell membranes resulting in leakage of cellular contents by cell disruption. This study reveals the potential of NiGs as an antimicrobial agent at 50 $\mu\text{g}/\text{mL}$ and hence could be exploited as antimicrobial coatings on surface of materials for various environmental and biomedical applications.

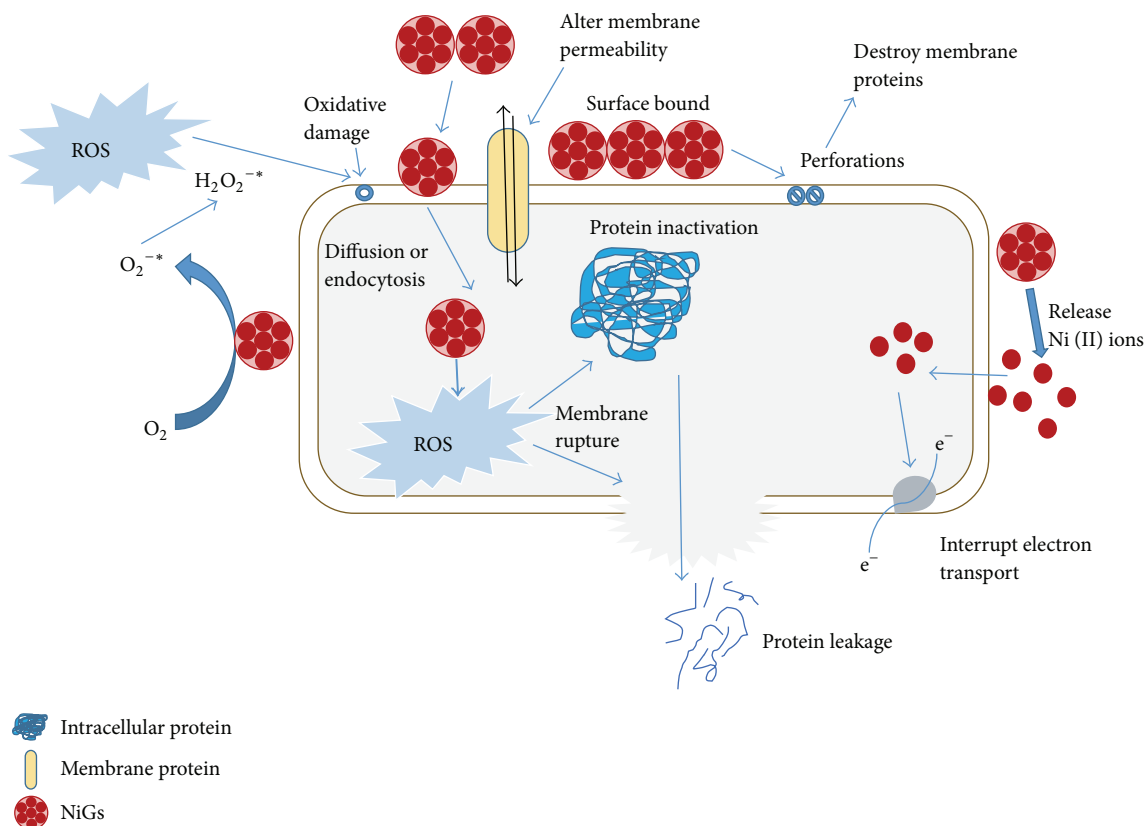


FIGURE 8: Mechanism of antimicrobial activity of green synthesized nickel nanoparticles.

Conflict of Interests

The authors declare that there is no conflict of interests regarding the publication of this paper.

References

- [1] Q. A. Pankhurst, N. K. T. Thanh, S. K. Jones, and J. Dobson, "Progress in applications of magnetic nanoparticles in biomedicine," *Journal of Physics D: Applied Physics*, vol. 42, no. 22, pp. 1–13, 2009.
- [2] J. R. Morones, J. L. Elechiguerra, A. Camacho et al., "The bactericidal effect of silver nanoparticles," *Nanotechnology*, vol. 16, no. 10, pp. 2346–2353, 2005.
- [3] S. Ravikumar, R. Gokulakrishnan, and P. Boomi, "In vitro antibacterial activity of the metal oxide nanoparticles against urinary tract infectious bacterial pathogens," *Asian Pacific Journal of Tropical Disease*, vol. 2, no. 2, pp. 85–89, 2012.
- [4] D. Liu, S. Ren, H. Wu, Q. Zhang, and L. Wen, "Morphology control in synthesis of nickel nanoparticles in the presence of polyvinylpyrrolidone (PVPK30)," *Journal of Materials Science*, vol. 43, no. 6, pp. 1974–1978, 2008.
- [5] A. R. Joseph and B. Viswanathan, "Synthesis of nickel nanoparticles with fcc and hcp crystal structures," *Indian Journal of Chemistry*, vol. 50, pp. 176–179, 2010.
- [6] S. Dhananasekaran, R. Palanivel, and S. Pappu, "Adsorption of methylene blue, bromophenol blue, and coomassie brilliant blue by α -chitin nanoparticles," *Journal of Advanced Research*, vol. 7, no. 1, pp. 113–124, 2016.
- [7] J. Huang, Q. Li, D. Sun et al., "Biosynthesis of silver and gold nanoparticles by novel sundried *Cinnamomum camphora* leaf," *Nanotechnology*, vol. 18, no. 10, Article ID 105104, pp. 105104–105115, 2007.
- [8] L.-C. Chiang, L.-T. Ng, P.-W. Cheng, W. Chiang, and C.-C. Lin, "Antiviral activities of extracts and selected pure constituents of *Ocimum basilicum*," *Clinical and Experimental Pharmacology and Physiology*, vol. 32, no. 10, pp. 811–816, 2005.
- [9] S. Jyoti, S. Satendra, S. Sushma, T. Anjana, and S. Shashi, "Antistressor activity of *Ocimum sanctum* (Tulsi) against experimentally induced oxidative stress in rabbits," *Methods and Findings in Experimental and Clinical Pharmacology*, vol. 29, no. 6, pp. 411–416, 2007.
- [10] C. Pellioux, A. Dewilde, C. Pierlot, and J.-M. Aubry, "Bactericidal and virucidal activities of singlet oxygen generated by thermolysis of naphthalene endoperoxides," *Methods in Enzymology*, vol. 319, pp. 197–207, 2000.
- [11] S.-H. Kim, H.-S. Lee, D.-S. Ryu, S.-J. Choi, and D.-S. Lee, "Antibacterial activity of silver nanoparticles against *Staphylococcus aureus* and *Escherichia coli*," *Korean Journal of Microbiology and Biotechnology*, vol. 39, no. 1, pp. 77–85, 2011.
- [12] C. J. Pandian, R. Palanivel, and S. Dhananasekaran, "Green synthesis of nickel nanoparticles using *Ocimum sanctum* and their application in dye and pollutant adsorption," *Chinese Journal of Chemical Engineering*, vol. 23, no. 8, pp. 1307–1315, 2015.
- [13] S. C. Yen and M. D. Mashitah, "Characterization of Ag nanoparticles produced by White-Rot Fungi and Its in vitro antimicrobial activities," *The International Arabic Journal of Antimicrobial Agents*, vol. 2, no. 3, pp. 1–8, 2012.

- [14] S. Gunalan, R. Sivaraj, and V. Rajendran, "Green synthesized ZnO nanoparticles against bacterial and fungal pathogens," *Progress in Natural Science: Materials International*, vol. 22, no. 6, pp. 693–700, 2012.
- [15] I. Sondi and B. Salopek-Sondi, "Silver nanoparticles as antimicrobial agent: a case study on *E. coli* as a model for Gram-negative bacteria," *Journal of Colloid and Interface Science*, vol. 275, no. 1, pp. 177–182, 2004.
- [16] G. Basak, D. Das, and N. Das, "Dual role of acidic diacetate sophorolipid as biostabilizer for ZnO nanoparticle synthesis and biofunctionalizing agent against *Salmonella enterica* and *Candida albicans*," *Journal of Microbiology and Biotechnology*, vol. 24, no. 1, pp. 87–96, 2014.
- [17] S. Arokiyaraj, M. V. Arasu, S. Vincent et al., "Rapid green synthesis of silver nanoparticles from *Chrysanthemum indicum* L and its antibacterial and cytotoxic effects: an in vitro study," *International Journal of Nanomedicine*, vol. 9, no. 1, pp. 379–388, 2014.
- [18] A. J. Kora and J. Arunachalam, "Assessment of antibacterial activity of silver nanoparticles on *Pseudomonas aeruginosa* and its mechanism of action," *World Journal of Microbiology and Biotechnology*, vol. 27, no. 5, pp. 1209–1216, 2011.
- [19] K. Mallikarjuna, G. Narasimha, G. R. Dillip et al., "Green synthesis of silver nanoparticles using *Ocimum* leaf extract and their characterization," *Digest Journal of Nanomaterials and Biostructures*, vol. 6, no. 1, pp. 181–186, 2011.
- [20] R. Govindasamy, R. Jeyaraman, J. Kadarkaraihangam et al., "Novel and simple approach using synthesized nickel nanoparticles to control blood-sucking parasites," *Veterinary Parasitology*, vol. 191, pp. 332–339, 2013.
- [21] X. S. Wang, X. Liu, L. Wen, Y. Zhou, Y. Jiang, and Z. Li, "Comparison of basic dye crystal violet removal from aqueous solution by low-cost biosorbents," *Separation Science and Technology*, vol. 43, no. 14, pp. 3712–3731, 2008.
- [22] A. K. Suresh, D. A. Pelletier, and M. J. Doktycz, "Relating nanomaterial properties and microbial toxicity," *Nanoscale*, vol. 5, no. 2, pp. 463–474, 2013.
- [23] H. F. Salem, K. A. M. Eid, and M. A. Sharaf, "Formulation and evaluation of silver nanoparticles as antibacterial and antifungal agents with a minimal cytotoxic effect," *International Journal of Drug Development and Research*, vol. 3, pp. 293–304, 2011.
- [24] K.-J. Kim, W. S. Sung, B. K. Suh et al., "Antifungal activity and mode of action of silver nano-particles on *Candida albicans*," *BioMetals*, vol. 22, no. 2, pp. 235–242, 2009.
- [25] W.-R. Li, X.-B. Xie, Q.-S. Shi, H.-Y. Zeng, Y.-S. Ou-Yang, and Y.-B. Chen, "Antibacterial activity and mechanism of silver nanoparticles on *Escherichia coli*," *Applied Microbiology and Biotechnology*, vol. 85, no. 4, pp. 1115–1122, 2010.
- [26] H. Pang, F. Gao, and Q. Lu, "Morphology effect on antibacterial activity of cuprous oxide," *Chemical Communications*, vol. 7, no. 9, pp. 1076–1078, 2009.
- [27] J. Sawai, "Quantitative evaluation of antibacterial activities of metallic oxide powders (ZnO, MgO and CaO) by conductimetric assay," *Journal of Microbiological Methods*, vol. 54, no. 2, pp. 177–182, 2003.
- [28] W. Lin, Y.-W. Huang, X.-D. Zhou, and Y. Ma, "Toxicity of cerium oxide nanoparticles in human lung cancer cells," *International Journal of Toxicology*, vol. 25, no. 6, pp. 451–457, 2006.
- [29] J. S. Kim, E. Kuk, K. N. Yu et al., "Antimicrobial effects of silver nanoparticles," *Nanomedicine: Nanotechnology, Biology, and Medicine*, vol. 3, no. 1, pp. 95–101, 2007.
- [30] S. Thirunavukkarasu, R. Abdul, J. Chidambaram et al., "Green synthesis of titanium dioxide nanoparticles using *Psidium guajava* extract and its antibacterial and antioxidant properties," *Asian Pacific Journal of Tropical Medicine*, vol. 7, no. 12, pp. 968–976, 2014.
- [31] M. Fang, J.-H. Chen, X.-L. Xu, P.-H. Yang, and H. F. Hildebrand, "Antibacterial activities of inorganic agents on six bacteria associated with oral infections by two susceptibility tests," *International Journal of Antimicrobial Agents*, vol. 27, no. 6, pp. 513–517, 2006.
- [32] O. Choi and Z. Hu, "Size dependent and reactive oxygen species related nanosilver toxicity to nitrifying bacteria," *Environmental Science and Technology*, vol. 42, no. 12, pp. 4583–4588, 2008.
- [33] K. Kenneth, Y. Wong, and L. Xuelai, "Silver nanoparticles—the real 'silver bullet' in clinical medicine," *Medicinal Chemistry Communications*, vol. 1, pp. 125–131, 2010.
- [34] R. K. Chrakanth, C. Ashajyothi, A. K. Oli, and C. Prabhurajeshwar, "Potential bactericidal effect of silver nanoparticles synthesised from *Enterococcus species*," *Oriental Journal of Chemistry*, vol. 30, no. 3, pp. 1253–1262, 2014.
- [35] S. Agnihotri, S. Mukherji, and S. Mukherji, "Size-controlled silver nanoparticles synthesized over the range 5–100 nm using the same protocol and their antibacterial efficacy," *RSC Advances*, vol. 4, no. 8, pp. 3974–3983, 2014.
- [36] Y. S. Chan and M. D. Mashitah, "Biosynthesis of silver nanoparticles from *Schizophyllum commune* and In-vitro antibacterial and antifungal studies," *Journal of Physical Science*, vol. 24, no. 2, pp. 83–96, 2013.
- [37] A. Nasrollahi, Kh. Pourshamsian, and P. Mansourkiaee, "Antifungal activity of silver nanoparticles on some of fungi," *International Journal of Nano Dimension*, vol. 1, no. 3, pp. 233–239, 2011.
- [38] A. Panáček, M. Kolář, R. Večeřová et al., "Antifungal activity of silver nanoparticles against *Candida* spp.," *Biomaterials*, vol. 30, no. 31, pp. 6333–6340, 2009.
- [39] C. Gao, Y. Xu, and C. Xu, "In Vitro activity of nano-silver against ocular pathogenic fungi," *Life Science Journal*, vol. 9, no. 4, pp. 750–753, 2012.
- [40] A. Monir and S. Azar, "Antifungal activity of silver nanoparticles indifferent sizes against some pathogenic fungi," *Journal of Applied Chemical Research*, vol. 8, no. 4, pp. 115–122, 2014.
- [41] J. Jain, S. Arora, J. M. Rajwade, P. Omray, S. Khandelwal, and K. M. Paknikar, "Silver nanoparticles in therapeutics: development of an antimicrobial gel formulation for topical use," *Molecular Pharmaceutics*, vol. 6, no. 5, pp. 1388–1401, 2009.



Hindawi

Submit your manuscripts at
<http://www.hindawi.com>

